INTERNATIONAL JOURNAL OF AUTOMOTIVE AND MECHANICAL ENGINEERING (IJAME)
ISSN: 2229-8649 e-ISSN: 2180-1606
VOL. 17, ISSUE 1, 7629 – 7647
DOI: https://doi.org/10.15282/ijame.17.1.2020.12.0567

ORIGINAL ARTICLE

Performance Analysis of Trihexyltetradecylphosphonium Chloride Ionic Fluid under MQL Condition in Hard Turning

A. Pandey, R. Kumar*, A.K. Sahoo, A. Paul and A. Panda

School of Mechanical Engineering, Kalinga Institute of Industrial Technology (KIIT),
Deemed to be University, Bhubaneswar-24, Odisha, 751024, India, Tel: +91-0674-6540805.

ABSTRACT – The current research presents an overall performance-based analysis of Trihexyltetradecylphosphonium Chloride [[CH3-(CH2)5]P(Cl)(CH2)13CH3] ionic fluid mixed with organic coconut oil (OCO) during turning of hardened D2 steel. The application of cutting fluid on the cutting interface was performed through Minimum Quantity Lubrication (MQL) approach keeping an eye on the detrimental consequences of conventional flood cooling. PVD coated (TiN/TiCN/TiN) cermet tool was employed in the current experimental work. Taguchi's L9 orthogonal array and TOPSIS are executed to analysis the influences, significance and optimum parameter settings for predefined process parameters. The prime objective of the current work is to analyse the influence of OCO based Trihexyltetradecylphosphonium Chloride ionic fluid on flank wear, surface roughness, material removal rate, and chip morphology. Better quality of finish (Ra=0.2 to 1.82 μm) was found with 1% weight fraction but it is not sufficient to control the wear growth. Abrasion, chipping, groove wear, and catastrophic tool tip breakage are recognized as foremost tool failure mechanisms. The significance of responses have been studied with the help of probability plots, main effect plots, contour plots, and surface plots and the correlation between the input and output parameters have been analysed using regression model. Feed rate and depth of cut are equally influenced (48.98%) the surface finish while cutting speed attributed the strongest influence (90.1%). The material removal rate is strongly prejudiced by cutting speed (69.39 %) followed by feed rate (28.94%) whereas chip reduction coefficient is strongly influenced through the depth of cut (63.4%) succeeded by feed (28.8%). TOPSIS significantly optimised the responses with 67.1 % gain in closeness coefficient.

ARTICLE HISTORY
Revised: 27th Sept 2019
Accepted: 19th Dec 2019

KEYWORDS
Hard turning; MQL; Ionic fluid; Cermet insert; Flank wear; TOPSIS.

NOMENCLATURE

MQL	minimum quantity lubrication	ζ	chip reduction coefficient
IL	ionic liquid	ϕ	approach angle
AISI	American Iron and Steel Institute	OCO	organic coconut oil
HRC	Rockwell hardness	PVD	physical vapour deposition
CNC	computerized numerical control	ANOVA	analysis of variance
TiN	titanium nitride	CCo	closeness coefficient
TiCN	titanium carbide nitride	R-Square	determination coefficient
ISO	international standards organization	R-square(pred)	predicted r-square
v	cutting speed (m/min)	R-Square(adj)	adjacent r-square
f	feed rate (mm/rev)	DF	degrees of freedom
d	depth of cut (mm)	MS	mean square
Ra	surface roughness (μm)	F	variance ratio
VBc	tool-flank wear (mm)	P	probability
MRR	material removal rate (g/s)	TOPSIS	technique for order of preference by similarity to ideal solution
t	chip thickness (mm)		

INTRODUCTION

The immense burden on the earth due to increasing population, consequently an increase in consumption of resources and degradation has not just commanded the manufacturing engineers to achieve sustainability in manufacturing. But also given the scope of exploring different cooling and lubrication approaches which have been assistance in achieving better performance in terms of parameters like surface finish, tool wear and chip reduction coefficient. The mineral oil-based flood cooling method being used in industries has many inadequacies that need immediate attention. Around 30% of the coolant used in machining has been estimated to be wasted through leakages in the delivery circuits, or later in cleaning the pipes.

*CORRESPONDING AUTHOR | R. Kumar | ramanujkumar22@gmail.com

Moreover, the inefficient removal and treatment processes finally end up as the contamination in a river contributing to water pollution [1]. Apart from being a burden to nature as industrial pollution, the cutting fluid is also a source of major health hazard to the operators which causes skin irritation, skin or lung cancer, loss of pulmonary function, acne, pneumonia [2-4]. Besides, these systems occupy a lot of floor space, and arrangements for storage, pumping, recycling, and refining has to be accommodated. Their disposal cost is getting higher due to tightening up of environmental laws [5].

Numerous studies were performed on the minimum quantity lubrication (MQL) as one of the recourses in the field of coolants used in machining, spraying very less quantity of coolant and levelled the optimum balance between the lubricants used. A better cutting performance, superior dimensional accuracy, decreased cutting temperature was achieved by using MQL, compared to conventional machining [6]. Weinert et al. have suggested that better productivity by better performance in lesser time can be achieved by using MQL method [7]. MQL was considered as a more effective cooling method at lower cutting speed as compared to higher cutting speed due to lower time available to remove accrued heat at higher cutting speed. The generated chips have plastic or bulk contact, which restricted the MQL coolant to arrive into the hot tool-chip contact zone [8]. Despite having an advantage of better thermal stability and lubrication property, MQL systems lack their functionality in cooling. This occurs due to evaporation of the oil micro-particles before reaching the cutting interface, especially in the materials where the cutting temperature was high leading to poor lubrication and cooling effect [9]. To overcome the problems being faced in MQL for machining hard to cut materials, additives such as nanoparticles have been proposed in many works. Ionic liquid (IL) was observed to be a lesser explored and very capable additive due to the following reasons [10-13]:

i. Low vapor pressure
ii. High thermal stability
iii. High oxidative stability
iv. Non-volatile and non-flammable
v. High load-bearing capacity
vi. Eliminates the usage of detergents, deformers, and antioxidants.

According to Goindi et al. [14], by addition of ILs as an additive to vegetable oil in minute quantities, a significant reduction in cutting forces and surface roughness were noticed. In another research work, Goindi et al. [15] utilised two different types of ILs which were fluorine and phosphonium based. It was found that fluorine-based ILs are more suited for high-speed machining condition while phosphonium-based ILs was more favourable at lower cutting speed machining. Further, it was observed that the higher viscosity of a lubricant leads to a better surface finish. Additionally, by adding 1-butyl-3-methylimidazolium hexafluorophosphate (BMIM-PF6) IL into deionized water, Davis et al. observed the 60% reduction in tool wear compared to the dry cutting environment and 15% compared to water-based MQL while machining titanium alloys.

Moreover, it was visualised that an enhancement in the surface roughness of 25% related to dry machining [16]. Addition of halogen-free IL as an additive in water abridged the coefficient of friction by greater than 70% when matched to water, and attributed a trifling wear rate of aluminium [17]. According to Sani et al. [18], machining of AISI 1045 steel under modified Jatropha oil with 10 % ammonium imide IL attributed a significant reduction in surface roughness (7%), cutting temperature (9%) and cutting force (12%) while 50% tool life improved compared to conventional synthetic ester MQL fluid. Gutnichenko et al. [19] utilised graphite nano-additives rapeseed vegetable oil through MQL in hard turning of 60 HRC tempered steel.

Tool-crater wear was more with nanoparticles mixed oil compared to neat vegetable oil due to a larger contact load acted on the tool-edge because of lower contact area between tool-top surface and chip. Fernando et al. [20] compared the machining performance under mineral oil-based metalworking fluid (MWF) and coconut oil-based MWF. Experimentally, it was found that the coconut oil-based MWF worked superiorly as cutting temperature and flank wear growth was lower than mineral oil-based MWF. Agrawal and Patil [21] compared the MQL machining performance under mineral oil and non-vegetable oil (aloe vera oil). With the use of aloe vera oil, 6.7 % reduction in surface roughness and 0.14% decrement in tool wear were achieved compared to mineral oil. De Souza et al. [22] examined that the Jatropha based cutting fluid attributed the improved machining action relative to canola and mineral oil-based cutting fluids at low as well as high cut feed. It was concluded that the vegetable oil-based fluids are an environmentally friendly and technically rich coolant which comes from biodegradable and renewable resources. Duc et al. [23] concluded that the turning performance of hard 90CrSi steel using carbide tool is enhanced under MQL assisted Al_2O_3 and MoS_2 nanofluid. Soybean oil-based Al_2O_3 nanofluid was recommended for the best quality finish. Dong et al. [24] found the superior quality of surface finish with 0.5 weight % of MoS_2 nanofluid MQL in hard machining of tool steel. Das et al. [25] utilised rice bran oil-based three different nanofluid samples like Al_2O_3, Cuo and Fe_2O_3 in MQL hard turning and performance of CuO nanofluid was best among others nanofluids succeeded by Fe_2O_3 and Al_2O_3 nanofluids. Nune and Chaganti [26] developed a new metalworking fluid and found the highest ratio of the volume of metal removed to flank wear compared to oil-based metalworking fluid at same cutting situations.

The literature review summarises that the MQL technique was successfully utilised in hard machining, but it was more suited for low-speed machining condition. Besides the MQL technique, coolant which is used through it also plays a vital role in machining. Therefore, various alternatives to coolants were utilised in recent years to improve machinability performances. Nowadays, the application of nanofluid using the MQL technique in hard machining becoming popular due to their favourable thermal properties. But at the same time, ionic fluid as an additive to base fluid or nanofluid is becoming a novel approach for hard or high-speed machining concern. 1-butyl-3-methylimidazolium hexafluorophosphate ionic liquid was popularly used for machining applications. Trihexyltetradecylphosphonium chloride ionic fluid is not yet used for hard machining and from the tribological point of view, it attributed the better lubrication and thermal effects. However, it is worth needed to utilise it as an additive to base oil for further utilisation as a coolant using the MQL technique in hard machining. In past works, ionic fluid was mostly used in canola oil, so the addition of ionic liquid into coconut oil is a novel method for hard machining concern. Considering these literature gap the objectives of the current work is as follows:

i. Synthesis of coconut oil based Trihexyltetradecylphosphonium chloride ionic fluid.
ii. Performance analysis of coconut oil-mixable ionic liquid as additives in hard turning of AISI D2 steel (59 ±1 HRC) using multi-layer coated cermet tool.
iii. Multi-response parametric optimisation using TOPSIS.
iv. Linear modelling of responses using the regression technique.

METHODOLOGY

The proper choice approach of cutting condition, work-piece, tool and design of experiment has significant importance for contribution in the analysis. Referring to cutting tool manufacturer's handbook, machining practices, and machine tool process range, the process parameters i.e. cutting speed (*v*), feed rate (*f*) and depth of cut (*d*) have been selected. L_9 Taguchi design was chosen for the experimental investigation under MQL environment, and cutting process parameter optimisation through TOPSIS were performed in this current analysis. An optimisation analysis was accomplished to determine the ideal cutting factors during MQL machining condition. Currently, there is insufficient research on the correlation between main cutting parameters and output parameter responses in MQL based turning processes with trihexyltetradecylphosphonium chloride as an additive lubricant. Therefore, a novel trihexyltetradecylphosphonium chloride [$[CH_3(CH_2)_5]P(Cl)(CH_2)_{13}CH_3$] (Figure 1) was used as an additive for the lubricant which was brought from Sigma Aldrich now Merck and shown in Figure 2. The phosphonium based cation was selected due to its excellent performance in tribology, inertness to organic oil, non-corrosive nature, miscibility, anti-wear, and anti-scuffing properties [27-31]. Additionally, effective results of halogen-based anions were noticed in the work [14-16, 32-34]. Studies by Fox and Priest suggested that similar ILs not containing fluorine were less effective as lubricants compared to hydrocarbons, especially in the reduction of wear on surfaces caused by tribo-corrosion [34].

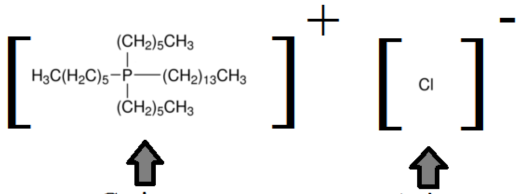

Figure 1. Trihexyltetradecylphosphonium chloride.

The material chosen for the experiment was AISI D2 Steel due to its wide range of application in die making, automotive and manufacturing industry and electronic industry. The cylindrical bars having a hardness level of (59±1) HRC with an original diameter of 46 mm and machining length of 170 mm were utilised. The turning process was performed on Jyoti DX200 CNC lathe with Fanuc controller, which encompasses high precision accuracy and up to 4000 RPM spindle speed capacity. Based on easy availability and extensive application of multilayer-coated (TiN/TiCN/TiN) cermet tool made by Kennametal was selected for machining purpose. A fresh insert was chosen in each run for the analysis of tool-flank wear. The industry-based MQL lubrication setup by DROPSA Germany was used in the current work. The detail of the experimental scheme is listed in Table 1.

The Taylor Hobson (Surtronic 25) surface roughness tester was calibrated with ISO 4287 standard before the surface roughness (Ra) measurement. The surface roughness measurement followed the ISO 3274-1996 standard. It was performed at five different places on the turned cylindrical work surface, and the arithmetic average was taken out. The roughness tester set up parameters like the number of sampling, cut off length and assessment length were 5 mm, 8 mm and 4 mm individually used during surface roughness measurement. The study of tool-flank wear, VBc, and chip morphology was carried out on Olympus STM6 optical microscope with image analysing software. The tool-flank wear was observed on a 50x optical zoom lens whereas the chips were studied on a 10x optical zoom lens. Material removal rate, MRR, was estimated experimentally using Eq. (1). Chip thickness, t, was estimated using a digital calliper and further chip reduction coefficient, ζ, was estimated by Eq. (2) [35-36].

$$MRR=\frac{(\text{Initialweight-finalweight})}{\text{Machiningtime}} \tag{1}$$

$$\zeta=\frac{t}{f.Sin\phi} \tag{2}$$

where, ϕ is approach angle.

Table 1. Experimental scheme.

Machining condition	Characteristics
Machine tool	11 kW power, make JYOTI, and model variants: DX 2004
Workpiece with hardness level and dimension	AISI D2 steel (59±1) HRC & D x L = 46 x 170 mm
Cutting tool	PVD multilayer coated (TiN/TiCN/TiN) cermet tool (KT 315) WIDIA Germany
Tool Geometry	Inclination angle -6º Negative rake angle -6º Clearance angle 6º Approach angle 95º Point angle 80º Nose radius 0.8 mm
Tool holder geometry	PCLNR2525M12
Lubricant	Trihexyltetradecylphosphonium chloride + coconut oil
Cutting speed (*v*) m/min	60, 120, 180
Feed (*f*) mm/rev	0.06, 0.12, 0.18
Depth of cut (*d*) mm	0.2, 0.3, 0.4
Cooling method	Minimum quantity lubrication (MQL)
lubrication setup	DROPSA make by Germany
MQL flow rate	20 ml/hr with compressed air
Measured parameters	Surface roughness, flank wear, material removal rate, chip reduction coefficient

Synthesis of Ionic Fluid

Organic coconut oil (OCO) was chosen as a base fluid in the current work. Trihexyltetra-decylphosphonium chloride of 1% weight was immersed into organic coconut oil and then appropriately mixed using the magnetic stirrer for around 1 hour as displayed in Figure 2 and, later was sonicated in an ultrasonic vibrator for 40 minutes. This phosphonium additive is hydrophobic in nature and fully soluble in coconut oil.

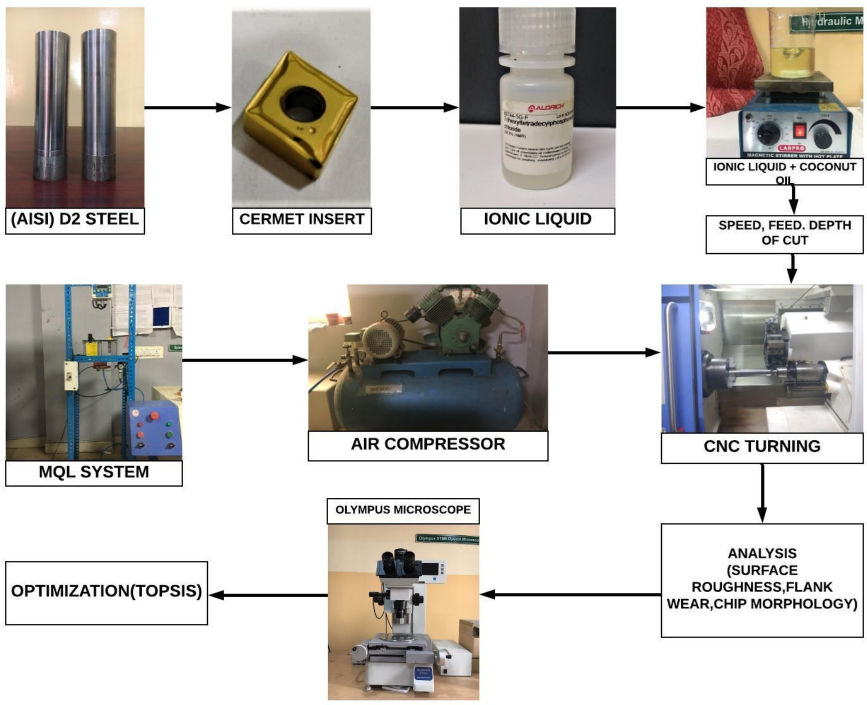

Figure 2. Experimental outline.

EXPERIMENTAL RESULTS

Taguchi L_9 experimental input code, actual inputs and experimental results for output responses namely surface roughness (Ra), tool flank wear (VBc), material removal rate (MRR) and chip reduction co-efficient (ζ) are presented in Table 2. The chip morphology, along with chip thickness, t, is listed in Table 3.

Table 2. Experimental data.

Run no.	L_9-coded inputs			L_9-actual inputs			Measured responses			
	d	*f*	*v*	*d* (mm)	*f* (mm/rev)	*v* (m/min)	Ra (µm)	VBc (mm)	MRR (g/s)	ζ
1	1	1	1	0.2	0.06	60	0.2	0.092	0.149	1.673
2	1	2	2	0.2	0.12	120	0.44	0.313	0.983	1.422
3	1	3	3	0.2	0.18	180	0.9	0.463	1.817	1.226
4	2	1	2	0.3	0.06	120	0.46	0.339	0.610	1.840
5	2	2	3	0.3	0.12	180	1.06	0.619	1.427	1.589
6	2	3	1	0.3	0.18	60	1.31	0.096	0.704	1.673
7	3	1	3	0.4	0.06	180	0.88	0.718	0.984	2.008
8	3	2	1	0.4	0.12	60	1.33	0.123	0.287	1.923
9	3	3	2	0.4	0.18	120	1.82	0.426	1.218	1.729

Analysis of Surface Roughness

Surface roughness is one of the important machinability criteria to measure the performance of machining process. It is not just a parameter used to judge the quality of machining but, also has a high influence on various properties such as wear resistance, corrosion resistance and fatigue strength of the finished surface. Hence, manufacturing industries strive to achieve a better surface finish, with higher productivity with lower cost [36]. The surface roughness in the experimental investigation has been ranged from 0.2 µm to 1.82 µm (Table 2), with mean of 0.93 µm and a standard deviation of 0.51 which is shown in probability graph of Ra (Figure 3). All experimental values are within the criterion limit of 1.6 µm except for Run no. 9 that can be treated as an exception due to catastrophic failure of tool insert at the highest cutting speed of 180 m/min [37-38]. Hence, the implementation of hard turning can be justified for the results being comparable to traditional grinding [36-41]. Also, the effects of the ionic liquid are clearly visible through numeric results of Ra as lowest value is 0.2 µm which is 3.1 times better than dry condition [36] and 2.7 times better than spray cooling condition [42]. Goindi et al. also found improved surface quality at 1 wt.% of phosphonium based ionic fluid [15]. From the literature, it can be stated that the current surface finish is better than the Ra values occurred in coconut oil and mineral oil machining. According to Belluco and De Chiffre [43], vegetable oil containing cutting coolant attributed to the enhanced quality of finish than mineral oil because of the lower magnitude of cutting force generation. Also, Fernando et al. [20] stated that the coconut oil-based cutting coolant gave a better quality of finish than mineral oil-based cutting coolant.

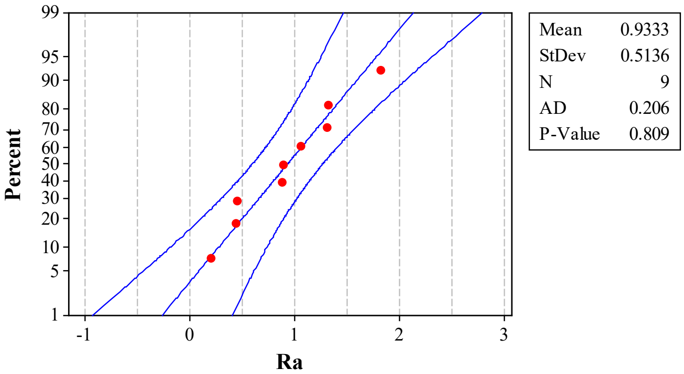

Figure 3. Probability distribution of Ra.

The strong consequence of depth of cut (*d*) and feed rate (*f*) can be observed on the Ra as displayed in Figure 4. Almost linear variation in Ra is noticed with respect to *d* and *f* while there is no effect of *v* on Ra has been seen as variation line lies onto the mean line. Similar trends were observed in the contour and surface plots of Ra (Figure 5). At the cutting terms *f* (0.06 mm/rev) with *v* (60 -80 m/min), Ra was found to be the least as shown by dark blue region in Figure 5(a). For low *v* and least *d* values, the Ra was found to be minimum, and it can be observed in Figure 5(b) that as the value of *d* increases surface finish decreases. A curvilinear graph was observed in Figure 5(c) where, with a low value of *f* and *d*, the Ra was found to be least. Therefore, it can be said that the surface finish was deteriorating with an increase in either individual or simultaneous values of term *f* and *d*. The surface plots in Figure 5(d) to (f) clearly show the dominancy of *f* and *d*, as the surface slope elevating with an increase in *f* and *d* values. In Figure 5(f) the surface is leading from both sides, which confirmed that the term *f* and *d* both are responsible for variation in Ra. Similar trends were reported by Kumar et al. [37].

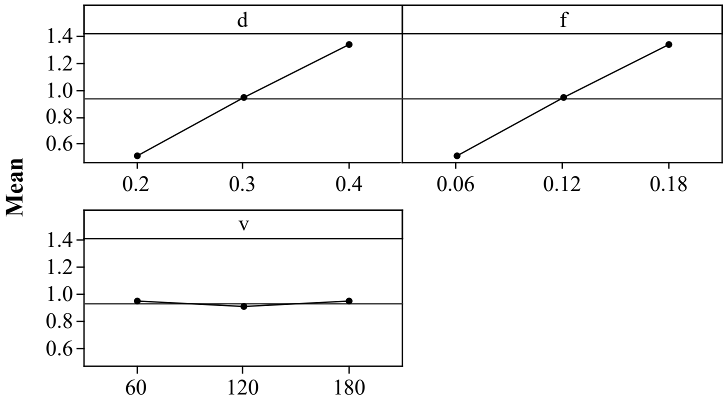

Figure 4. Effects of input terms on Ra.

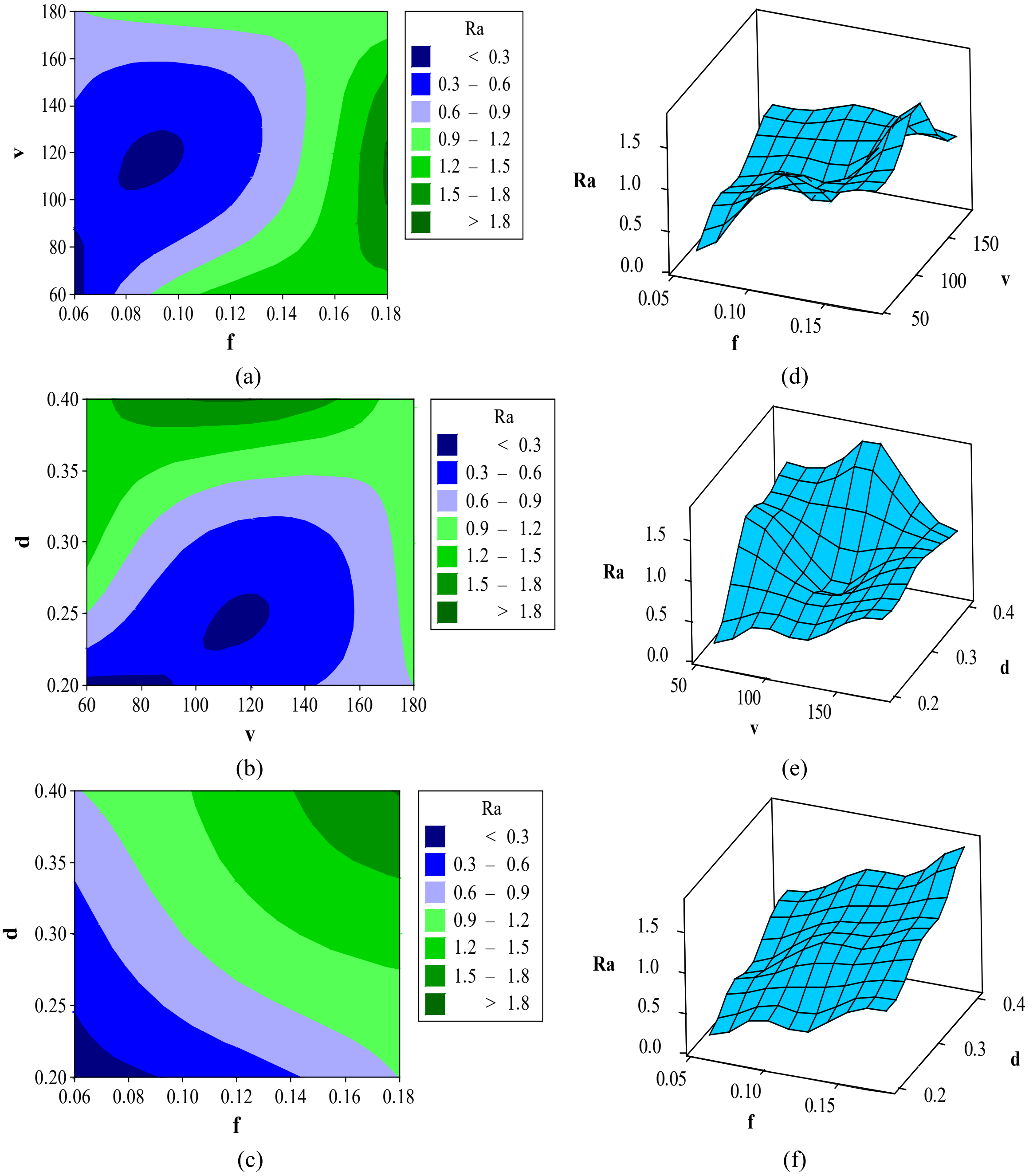

Figure 5. (a)-(c) Contour plot and (d)-(f) surface plot of Ra responding to parameters.

Similarly, from ANOVA in Table 4, the Ra is equally influenced by feed and depth of cut as their % contributions are same 48.98 %, and it also confirmed through main effect plot where curve line for both terms *f* and *d* are similar.

According to Yousefi and Zohoor, surface finish is mostly affected through feed rate (60%) and tool nose radius (28%) [44]. Depth of cut is also equally significant for Ra because the penetration depth is restricted through radial force in hard turning, especially when negative rake tool was used. However, the contribution of the depth of cut on Ra is the highest and is the same as feed due to its penetration in radial direction. As a result, the shear angle, friction and cutting force are larger, which deteriorated the surface finish [45]. An effect of cutting speed is not significant as their % contribution is almost negligible. However, it can be said that the influence of feed and depth of cut on Ra are equal; hence both are significant while cutting speed is insignificant.

Analysis of Flank Wear

A cutting tool is the most important element of a machining operation as it provides the finished component of the required shape, size, and tolerance by removing the unwanted material in the form of chips. In addition, tool flank wear during the machining is a very vital parameter to judge the nature of machining. Any manufacturing industry always strives to maximise the tool lifespan to achieve better profitability during the machining operation. As given in Table 2, the tool flank wears (VBc) ranges from 0.092 mm to 0.718 mm with the mean of 0.35mm and standard deviation of 0.22 as shown in Figure 6. The wear results confirmed that the particular machining is favourable when cutting speed is 60 m/min and beyond it flank wear is higher than the standard limit of 0.3 mm [36-38, 40-42]. Machining with 120 m/min, flank wear seems to be close to 0.3 mm (except at higher depth of cut = 0.3 mm). Therefore, 120 m/min speed might be used for other terms, namely Ra, MRR and ζ. Ionic fluid with 1% weight concentration is not might be suitable as wear value is found be in a higher range. Therefore, other concentrations may be useful and need to be used to check the wear growth.

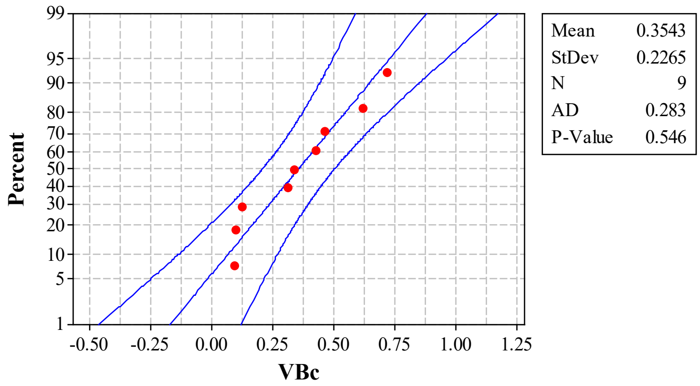

Figure 6. Probability distribution of VBc.

According to Goindi et al. [15], the use of higher weight concentration of oil-mixable ionic fluid may improve the machining performance under heavy machining condition. Current results confirmed a better performance than previously used mineral oils, and it is in agreement with literature published. According to Fernando et al. [20], coconut oil-based MWF attributed the lower values of flank wear relative to mineral oil-based MWF during machining of AISI 304 steel at cutting speed of 0.1 ms^{-1}. Also, Belluco and De Chiffre stated that the vegetable oil-based cutting coolant outperforms compared to mineral oil-based coolant as tool life was enhanced by 177% under vegetable oil compared to mineral oil [43]. Wear mechanism can be categorized as abrasion along with fine grooves at machining with 60 m/min as shown in Figure 7(a) while abrasion, chipping, plastic deformation are dominant on 120 m/min of machining as visible in Figure 7(b). Abrasion, chipping and catastrophically tool-tip breakage were noticed at the highest speed of 180 m/min of machining as shown in Figure 7(c). The feed is not contributed any significant role on VBc while leading depth of cut increases the wear rate. The heat affected marks are also clearly visible on to the tool-tip as displayed in Figure 7(a) to (c), and it may happen due to burning of coconut oil at high temperature.

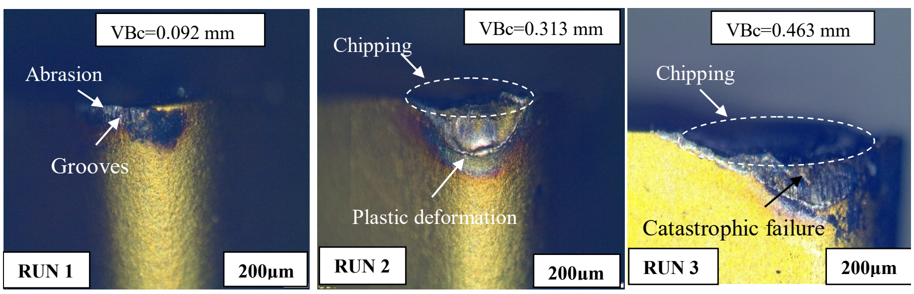

Figure 7. Optical-microscopic image of tool-flank wear.

The flank wear main effects plot (Figure 8) indicates that the cutting speed (*v*) has a significant relation of direct proportionality with the VBc. At the same time, the influence of *d* and *f* are marginal as the slope of the graph line is very less close to mean line. However, it can be summarised that only *v* is dominating the flank wear while *d* and *f* are insignificant. The contour plot of VBc as displayed in Figure 9(a) to (c) also suggested that VBc increased with the value of *v*, but *f* and *d* had very little influence on VBc. The surface plots displayed in Figure 9(d) to 9(e) indicates the gradual increment in surface-slope when *v* increases, while the effects of *d* and *f* are negligible. From Figure 9(f) the surface pattern is uneven, so the effects of *d* and *f* are not significant and considerable. ANOVA (Table 4) confirms that the cutting speed has the highest impact on VBc with highest and significant contribution of 90.1% while remaining term *d* and *f* are insignificant as their contributions are 4.6% and 1.09% correspondingly [42].

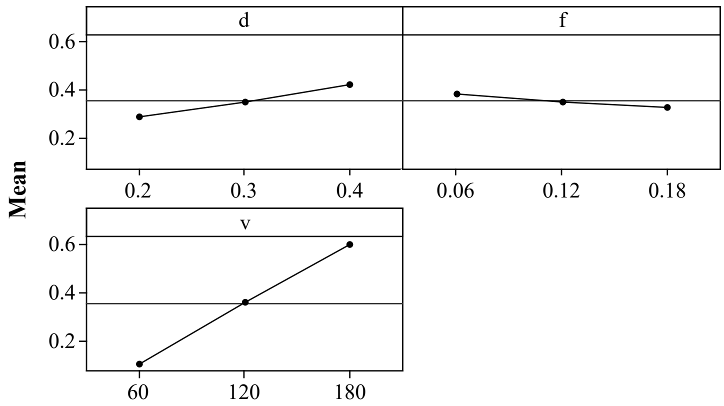

Figure 8. Effects of input terms on VBc.

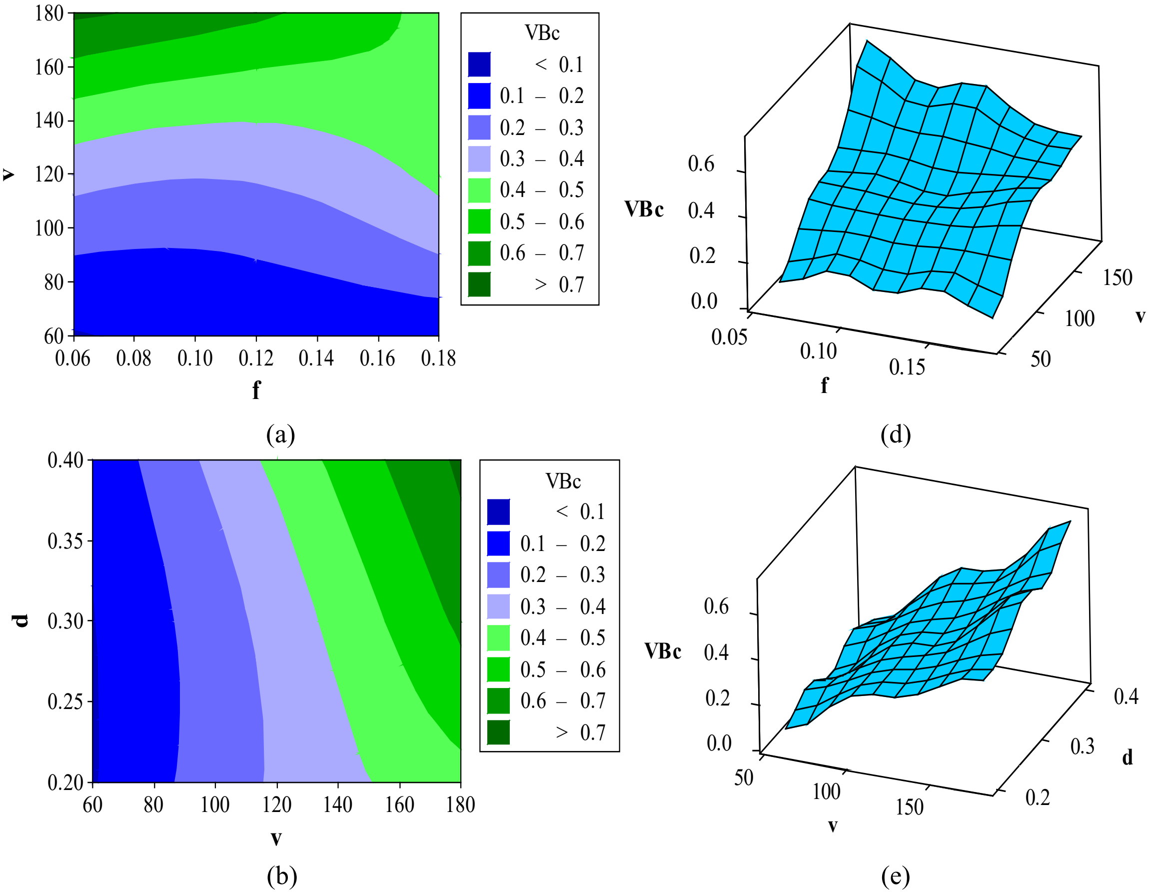

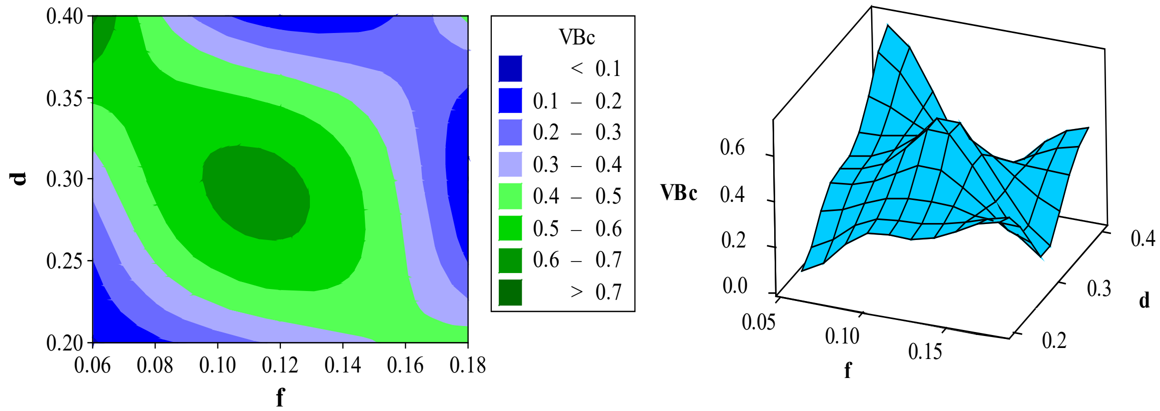

(c) (f)

Figure 9. (a)-(c) Contour plot and (d)-(f) surface plot of VBc responding to parameters.

Analysis of Material Removal Rate

The material removal rate is the amount of material reduced from a workpiece in the form of chips in the process of machining, which is desired to be high in any industry to cope up with the pressure of mass production and reach out the target in time. Higher MRR requires higher magnitudes of feed rate, depth of cut and cutting speed [46] but, as observed earlier high depth of cut and feed rate lead to an increment in surface roughness which isn't desirable. Hence, there is a critical need for balancing all the parameters to attain maximum productivity and profitability. From the test results (Table 2), the MRR ranges from 0.149 g/s to 1.427 g/s with an average of 0.908 g/s and deviation of 0.533 (Figure 10).

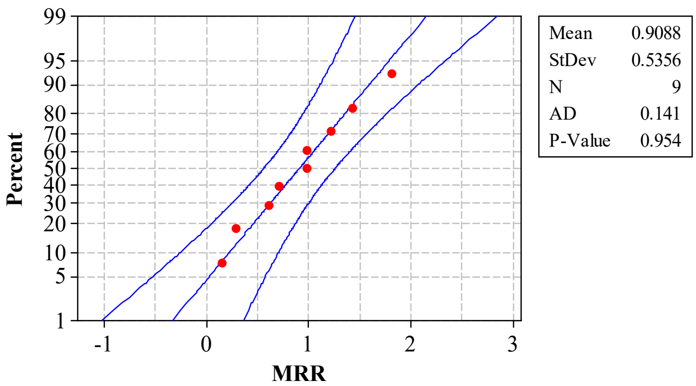

Figure 10. Probability distribution of MRR.

The main effect plot in Figure 11 clearly indicates the linear increment in MRR when *v* and *f* increasing, which suggests that both terms have a significant effect on the MRR. As the variation in *d* values (0.2 to 0.4 mm) is marginal, therefore, its effect on MRR is negligible, and it is also confirmed through main effect plot where with an increase in *d*, MRR isn't varied much. Among *v* and *f*, the influence of *v* on MRR is higher as their curve slope is higher than *f*. According to Mukherjee, MRR is significantly influenced by speed and feed [46]. From the contour plot displayed in Figure 12(a), it can be observed that the higher value of *v* and *f* correspond to higher MRR as denoted by green colour. From Figure 12(b) to 12(c), a higher MRR is noticed at a higher *f* and *v*, but influence of *d* is almost minute which represents insignificant effect on MRR. Surface plots as displayed in Figure 12(d) to 12(e) also confirmed the significant effect of *v* and *f* on MRR as surface-slope is increasing with increment in *v* and *f* values, whereas *d* doesn't attribute any significant change in MRR.

ANOVA (Table 4) indicates that the term *v* has highest significance on MRR as its highest contribution 69.39 % among others *d* and *f*. Further, influence of *f* on MRR is also significant as its contribution (28.94 %) is the second-highest while contribution of *d* on MRR is marginal (1.51%) which confirm the insignificant influence on MRR.

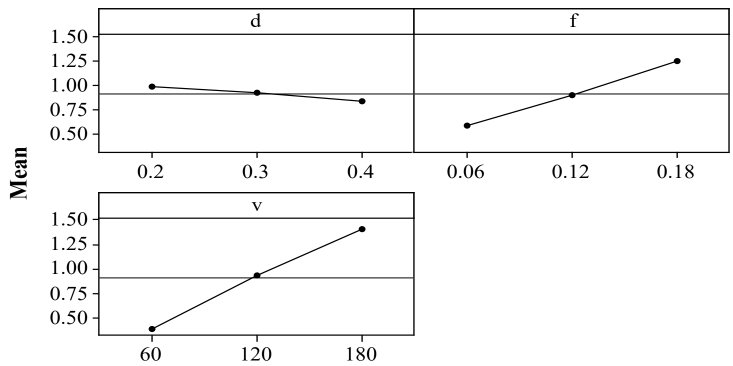

Figure 11. Effects of input terms on MRR

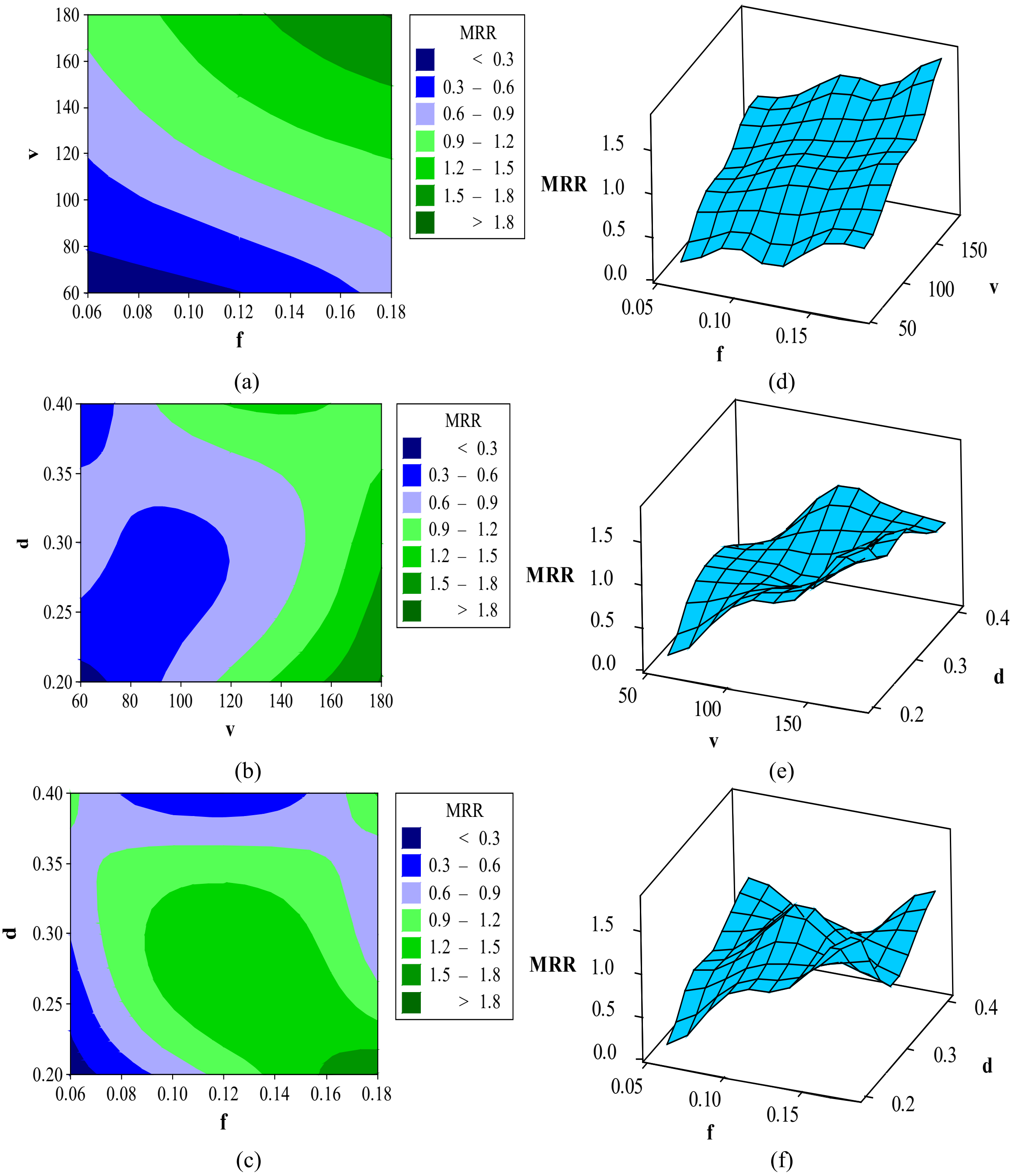

Figure 12. (a)-(c) Contour plot and (d)-(f) surface plots of MRR responding to parameters.

Analysis of Chip Morphology

Despite being the primary waste of machining in the industry, chip is of great value in the study of machining. Table 3 presents the overall morphology of chips (colour shape and chip thickness) formed during machining. A range of chips having different shapes, sizes and colours was observed. Sawtooth chips were noticed in each test due to cyclic fracture of material while cutting (Figure 13). Relatively, the smaller size of chips seen due to a lower tensile strain on the exterior surface of chips during bending by improved convective heat transfer coefficient. Thus, augment the cooling speed of the IL [47]. Considering parametric influence, the chip shape is highly affected by feed rate [37]. At lowest feed 0.06 mm/rev (run 1, 4 and 7) the shape of chips is coiled and continuous with helical shape. With the lowest depth of cut and moderate feed (run 2), the shape of the chip is coiled and continuous with helical shape. Continuous with ribbon shape chips are noticed at higher feed and cutting speed with the lowest depth of cut (run 3). On higher depth of cutting range (0.3-0.4 mm) with moderate feed (0.12 mm/rev) conditions, the continuous with ribbon shape chips are noticed (run 5 and 8). Broken with c-shape chips are perceived at the largest feed rate (0.18 mm/rev) condition as displayed in Figure 13(c). Similar observations were reported by Kumar et al. [37, 48-49].

Colour of chips is directly influenced by cutting temperature and cutting temperature is increasing with cutting speed. Therefore, it can be stated that the colour of chips are highly influenced by cutting speed and it is confirmed through chips morphology result. On maximum cutting speed (180 m/min) condition, the colour of chips is blue, while at the lowest speed, the colour of chips is metallic. At moderate speed (120 m/min) with moderate feed (0.12 m/min), the colour of chips is metallic. On the maximum depth of cut with the highest feed and moderate speed (run 9) the colour of chip is blue. Blue colour chips indicated the generation of intense cutting temperature although the ionic fluid is impinged on to the cutting zone due very short time available to penetrate the cutting fluid in the cutting zone [50]. It also confirms the higher friction value during machining, which attributed the poor surface finish and higher tool wear. The metallic colour is favourable for machining and it confirms the generation of lower intensity of cutting temperature due to a lower and moderate speed used under effective ionic fluid MQL cutting. Comparatively lower chip thickness is found by lowering the thermal stresses on to the tool-work-chip sliding surfaces due to efficient cooling capability of IL [47]. Experimentally (Table 3), it is identified that the chip thickness is growing with feed. Therefore, feed is the most influencing term for chip thickness concern.

Table 3. Details of chip morphology.

Run No.	Colour of chips	Shape of chips	Chip thickness (mm)
1	Metallic	Coiled and continuous with helical shape	0.10
2	Metallic	Coiled and continuous with helical shape	0.17
3	Blue	Continuous with ribbon shape	0.22
4	Metallic	Coiled and continuous with helical shape	0.11
5	Blue	Continuous with ribbon shape	0.20
6	Metallic	Broken with c-shape	0.28
7	Blue	Coiled and continuous with helical shape	0.12
8	Metallic	Continuous with ribbon shape	0.23
9	Blue	Broken with c-shaped	0.31

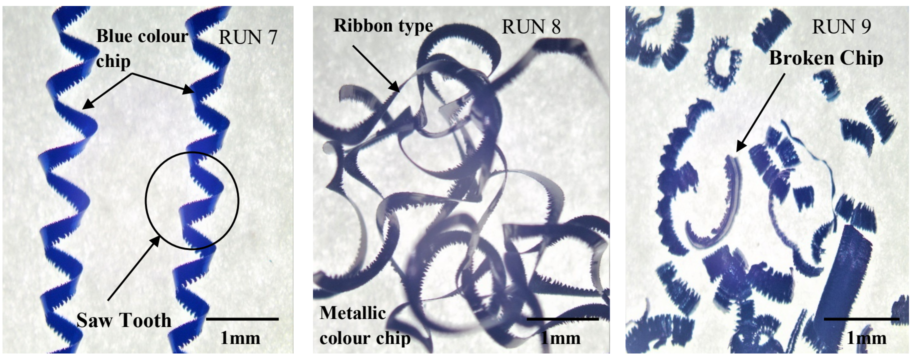

Figure 13. Different chip colours and shapes.

Chip reduction coefficient (ζ) is a ratio of the chip thickness before and after machining, which indicates the performance measure. In fact, ζ gives a qualitative indication of the power and specific energy utilised in the cutting process [36, 48-49]. The mean CRC for the nine runs was found to be around 1.655 with a standard deviation of 0.245 (Figure 14) which shows the efficient machining under ionic fluid condition. The main effect plot in Figure 15 suggests that ζ has a strong dependency on d and f as ζ increases with d and reduces with f at higher rate. Whereas, dependency on v was found to be comparatively lesser as the rate of decrement in ζ is lower. However, d and f are significant terms towards ζ while v is insignificant. Similarly from the contour plot as displayed in Figure 16(a) to (c), ζ is largely dominant by d and f terms, while the influence of v is relatively low. Higher ranges of ζ have been seen with higher values of d and lower values of *f* and *v*. Further, from Figure 16(d), a higher ζ is noticed with lower *f* and higher *v* conditions while uneven variations are noticed in other interaction values of *f*-*v*. From Figure 16(e), the ζ surface slope reducing with leading v and reducing d while at lowest v and highest d, ζ is highest. Similarly, from Figure 16(f), a diagonal surface is noticed which attributes the significance effect of *d*-*f* interaction on ζ. Therefore, the ζ is mainly influenced by the terms *d* and *f*. ANOVA in Table 4 indicates terms *d* and *f* are significant with the highest contribution of depth of cut (63.4 %) succeeded by feed (28.8 %), while cutting speed is insignificant as their contribution (7.1 %) is lowest. Similar trends were reported by Kumar et al. [36, 38-39, 42, 48-49]. The above statics ensure that the higher cutting force generation with an increase in depth of cut and feed during the cutting process and produces poor quality of finish as shown in result Table 2.

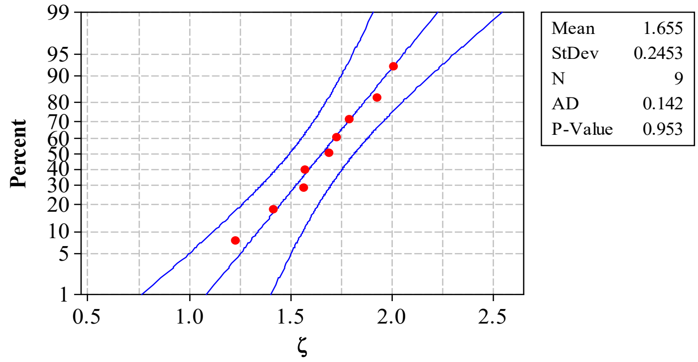

Figure 14. Probability distribution of ζ.

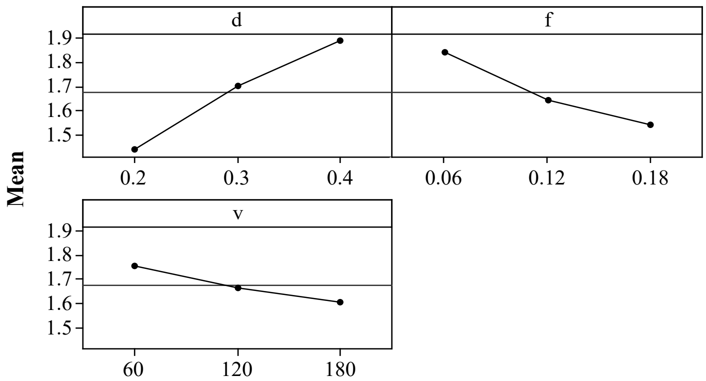

Figure 15. Effects of input terms on ζ.

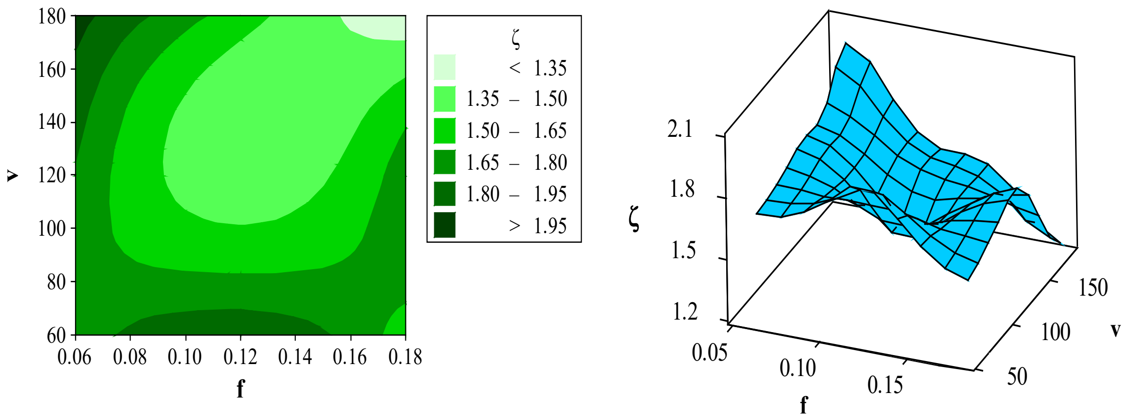

(a) (d)

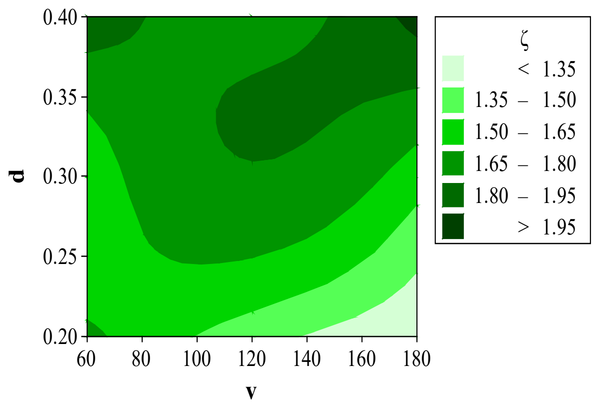

(b)

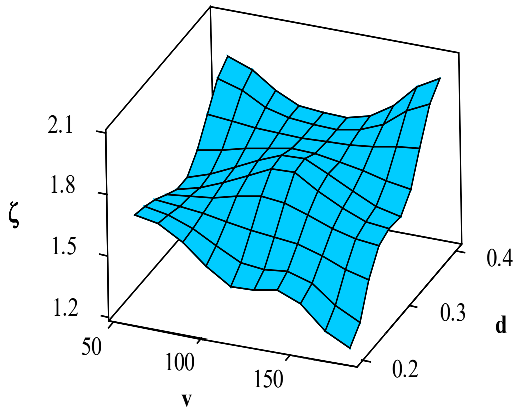

(e)

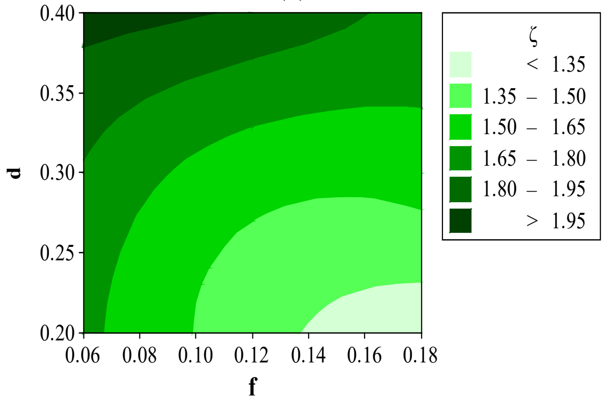

(c)

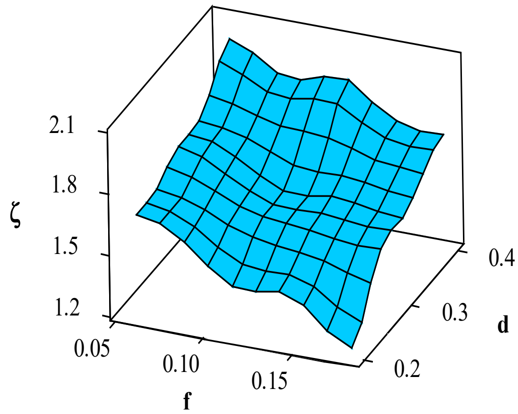

(f)

Figure 16. (a)-(c) Contour plot and (d)-(f) surface plot of ζ responding to parameters.

Table 4. ANOVA results

Source	DF	SS	MS	F	P	Contribution	Remark
Ra							
d	2	1.0338	0.5169	25.97	0.037	48.98 %	Significant
f	2	1.0338	0.5169	25.97	0.037	48.98 %	Significant
v	2	0.0032	0.0016	0.08	0.926	0.15 %	Insignificant
Error	2	0.0398	0.01990			1.89 %	Insignificant
Total	8	2.1106					
		S = 0.141067	R-Square = 98.11 %		R-Square(adj) = 92.46 %		
VBc							
d	2	0.0265	0.0132	2.79	0.264	6.46 %	Insignificant
f	2	0.0045	0.0022	0.47	0.679	1.09 %	Insignificant
v	2	0.3696	0.1848	38.75	0.025	90.1 %	Significant
Error	2	0.0095	0.0047			2.35 %	Insignificant
Total	8	0.4102					
		S = 0.0690604	R-Square = 97.67 %		R-Square(adj) = 90.70 %		
MRR							
d	2	0.0353	0.0176	13.62	0.068	1.53 %	Insignificant
f	2	0.6644	0.3322	255.79	0.004	28.94 %	Significant
v	2	1.5928	0.7964	613.22	0.002	69.39 %	Significant
Error	2	0.0026	0.0013			0.14 %	Insignificant
Total	8	2.2952					
		S = 0.0360386	R-Square = 99.89 %		R-Square(adj) = 99.55 %		
ζ							
d	2	0.3015	0.1507	106.26	0.009	63.4 %	Significant
f	2	0.1373	0.0686	48.37	0.020	28.8 %	Significant
v	2	0.0338	0.0169	11.92	0.077	7.1 %	Insignificant
Error	2	0.0028	0.0014			0.7 %	Insignificant
Total	8	0.4755					
		S = 0.0376711	R-Square = 99.40 %		R-Square(adj) = 97.61 %		

Topsis Multi-Response Optimisation

Among various multi-response optimisation methods, TOPSIS is chosen, which is based on the idea that the alternative chosen should be the shortest geometric distance from the positive ideal solution (PIS) [51]. It is based on the idea of positive and negative ideal value such that all the values should be between the maximum and minimum value limit. It not only gives the best outcome (maximum value) but also the worst outcome (minimum value). Closeness co-efficient is derived to find out the best and worst-performing result [51-53]. TOPSIS is considered simple and believed to be more expressible than other multi-response optimisation methods. In this current article, the objective of the TOPSIS method is to convert multi-response data into a single response data by evaluating the four outcomes such as Ra, VBc, MRR and ζ. The mathematical process for TOPSIS is shown stepwise in Eq. (3)-(6) as follows [51-53]:

Step 1: Initial matrix depending on the number of alternative and criteria. Suppose there are r alternatives and y criteria in a matrix $A_x = (x)_{x\,r\,y}$

$$A_x = \begin{array}{c|ccc} & C1 & C2 & \ldots Cy \\ \hline A1 & x11k & x12k & \ldots x1ky \\ A2 & x21k & x22k & \ldots x2ky \\ \ldots & \ldots & \ldots & \ldots\ldots.. \\ Ar & xrk1 & xrk2 & \ldots xryk \end{array}$$

Step 2: Normalisation of matrix using Eq. (3).

$$A_x = \frac{M_{ij}}{\sqrt{\sum_{i=1}^{n} M_{ij}}} \tag{3}$$

Where i=1,2,…..n; j=1,2,…..m, M_{ij} is the actual value of the i[th] value of j[th] experimental run and A_x is the normalised value.

Step 3: Normalised value matrix is converted into weighted value matrix by multiply with reciprocal of the number of criteria i.e.; (1/4=0.25)

Step 4: The ideal best value (A^+) and ideal worst value (A^-) is calculated by selecting the suitable value against the respective criteria. The ideal best for MRR will be the highest value from the weighted matrix and low value for ideal worst. The ideal best for Ra, VBc, and ζ will have the corresponding lowest value and similarly, the highest value represents ideal worst.

Step 5: Calculating the Euclidean distance ϵ^+ and ϵ^- from the ideal best and ideal worst values as noted in Eq. (4) and (5)

$$\epsilon^{+} = [\sum_{j=1}^{r} (A_{ij} - A_j^{+})^2]^{0.5} \tag{4}$$

$$\epsilon^{-} = [\sum_{j=1}^{r} (A_{ij} - A_j^{+})^2]^{0.5} \tag{5}$$

Step 6: Closeness coefficient (CCo) is calculated by the following Eq. (6).

$$CCo = (\epsilon^- / \epsilon^- + \epsilon^+) \tag{6}$$

The closeness coefficient is used to grade the alternative with greater value graded 1 and so on graded in the ascending order [51, 53]. Initially, the experimental results are arranged in an input matrix (Table 5). From this result, the normalised matrix is developed by using Eq. (3) and mentioned in Table 5. The response MRR is taken as higher is better, while other responses Ra, VBc and ζ are taken as lower is better criteria [48, 49]. The weighted matrix is prepared to form normalised matrix data by multiplying their individual data with reciprocal of the number, i.e. (1/4=0.25) and shown in Table 6. From step 4, the positive ideal solution (V_j^+) for MRR is the largest value, and for Ra, VBc and ζ are the lowest value. Similarly, a negative ideal solution (V_j^-) for MRR is the lowest value, and for other responses, namely Ra, VBc and ζ are the largest value. Ideal best and worst value for each response is noticed in Table 7. Euclidean distance ϵ^+ and ϵ^- has been estimated using Eq. (4) to (5) and displayed in Table 8. Further, CCo (closeness coefficients) are estimated using Eq. (6) and noted in Table 8. The CCo-rank is estimated according to their results data. Highest CCo indicates the best combination of input setting of parameters among the others [51-52]. Also, mean CCo is estimated as shown in Table 9 and from this higher mean value of each individual term represents their optimum level. From this the optimum level of parameters are *d*1(0.2 mm) -*f*2(0.12 mm/rev)-*v*2(120 mm/rev) as shown in Table 9. From the rank of mean CCo (Table 9), depth of cut corresponds to the first rank followed by speed and feed. However, the depth of cut exhibits the highest influence on CCo succeeded by speed and feed. Further, from confirmation run at optimal condition *d*1(0.2 mm) -*f*2(0.12 mm/rev) - *v*2(120 mm/rev), the gain in closeness coefficient from initial setting *d*3(0.4 mm) - *f*1(0.06 mm/rev) - *v*3(180 m/min) is found as 0.261 i.e 67.1% more gain in CCo.

Table 5. Actual and normalised data.

Run	Actual result data				Normalised result data			
	Ra (μm)	VB_C (mm)	MRR (g/s)	ζ	Ra (μm)	VB_C (mm)	MRR (g/s)	ζ
1	0.2	0.092	0.149	1.673	0.063	0.074	0.047	0.329
2	0.44	0.313	0.983	1.422	0.139	0.252	0.315	0.280
3	0.9	0.463	1.817	1.226	0.285	0.373	0.582	0.241
4	0.46	0.339	0.610	1.840	0.145	0.273	0.195	0.362
5	1.06	0.619	1.427	1.589	0.336	0.498	0.457	0.313
6	1.31	0.096	0.704	1.673	0.415	0.077	0.225	0.329
7	0.88	0.718	0.984	2.008	0.278	0.578	0.315	0.395
8	1.33	0.123	0.287	1.923	0.421	0.099	0.092	0.378
9	1.82	0.426	1.218	1.729	0.576	0.343	0.390	0.340

Table 6. Weighted matrix.

Run	Ra (μm)	VB_C (mm)	MRR (g/s)	ζ
1	0.016	0.018	0.012	0.082
2	0.035	0.063	0.079	0.070
3	0.071	0.093	0.146	0.060
4	0.036	0.068	0.049	0.091
5	0.084	0.124	0.114	0.078
6	0.103	0.019	0.056	0.082
7	0.069	0.144	0.079	0.099
8	0.105	0.024	0.023	0.095
9	0.144	0.086	0.097	0.085

Table 7. Ideal best and worst value.

	Ra (μm)	VB_C (mm)	MRR (g/s)	ζ
$\mathbf{v_j^+}$	0.016	0.018	0.146	0.060
$\mathbf{V_j-}$	0.144	0.145	0.012	0.099

Table 8. Eucledion distance (ϵ^+, ϵ^-) and closeness coefficient (CCo).

ϵ^+	0.136	0.0831	0.093	0.115	0.131	0.127	0.157	0.156	0.155
ϵ^-	0.181	0.155	0.165	0.137	0.122	0.140	0.100	0.127	0.105
CCo	0.572	0.650	0.640	0.545	0.482	0.524	0.389	0.448	0.404
Rank	3	1	2	4	6	5	9	7	8

Table 9. Mean data of CCo.

Input terms	Level of input terms			Maximum - Minimum	Optimal settings	Rank
	1st level	2nd level	3rd level			
d	0.620	0.517	0.413	0.207	*d*1	1
f	0.502	0.526	0.522	0.004	*f*2	3
v	0.514	0.533	0.503	0.030	*v*2	2

Table 10. Confirmation test table.

Responses	Initial setting	Predicted setting	Optimal setting
	*d*3-*f*1-*v*3	*d*1-*f*2-*v*2	*d*1-*f*2-*v*2
Ra (μm)	0.880		0.440
VBc (mm)	0.718		0.313
MRR (g/s)	0.984		0.983
ζ	2.008		1.412
Closeness coefficient (CCo)	0.389	0.644	0.650
Gain in CCo	0.261		

Linear Regression Modelling

Linear regression models have been established to correlate the functional relationship between response and input terms [37, 48]. The regression approach through Minitab 16 software is used to develop the following linear models as in Eq. (7) to Eq. (10).

$$VBc = -0.286833 + 0.665\,d - 0.455556\,f + 0.00413611\,v \tag{7}$$
R-Square = 97.63%, R-Square(adj) = 96.21%, R-Square(pred) = 90.59%

$$Ra = -1.14167 + 4.15\,d + 6.91667\,f + 0.00000\,v \tag{8}$$
R-Square = 97.92%, R-Square(adj) = 96.67%, R-Square(pred) = 92.74%

$$MRR = -0.555889 - 0.766667\,d + 5.54444\,f + 0.00857778\,v \tag{9}$$
R-Square = 99.71%, R-Square(adj) = 99.53% and R-Square(pred) = 98.93%

$$\zeta = 1.45272 + 2.23167\,d - 2.48056\,f - 0.00123889\,v \tag{10}$$
R-Square = 97.76%, R-Square(adj) = 96.41%, R-Square(pred) = 92.25%

From the summary of all models, R-Square, R-Square(adj) and R-Square(pred) values are near about 100 %, which confirms that the developed model for responses VBc, Ra, MRR and ζ are significant and efficiently co-related the input terms with output parameters. Further, from the normal probability plots of each response (Figure 17), the residuals lie near around the fitted line which remarked that the developed models are well fitted and significant.

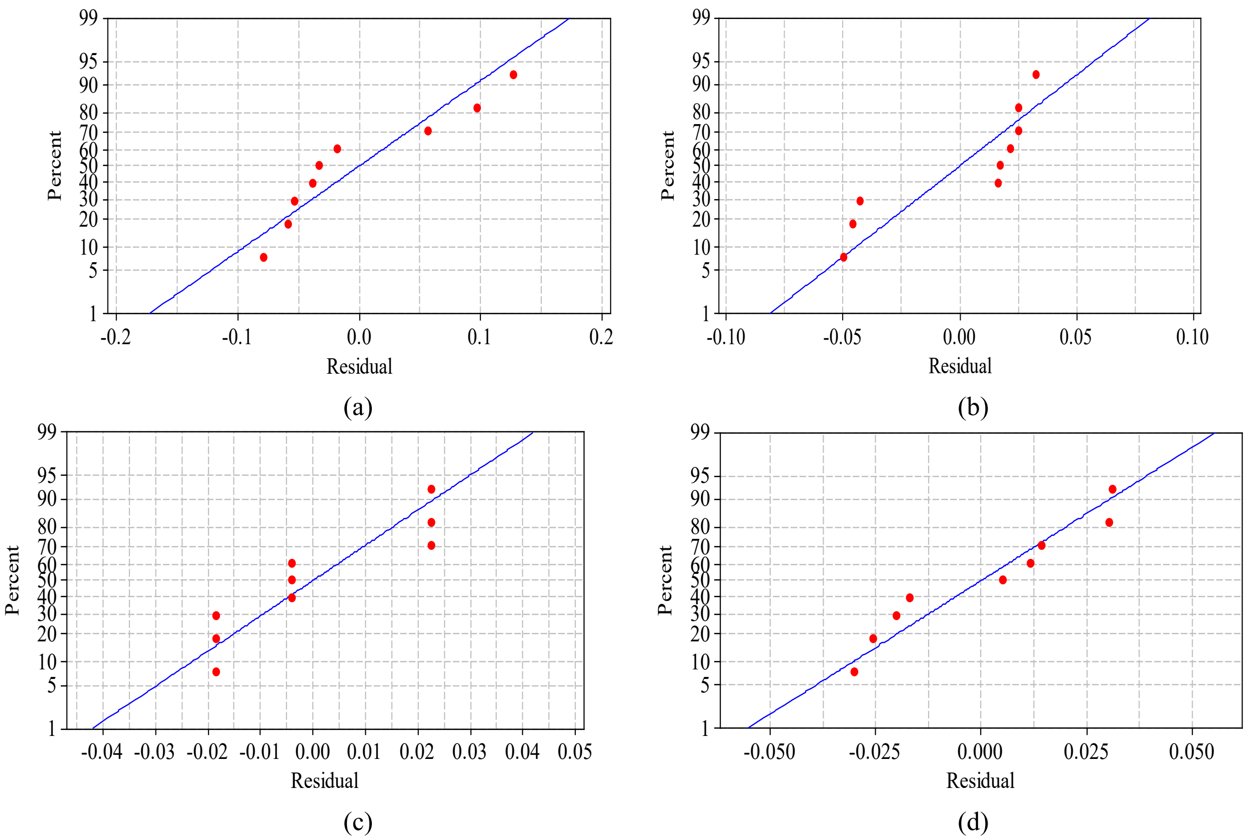

Figure 17. Normal plot for response (a) VBc (b) Ra (c) MRR (d) ζ.

CONCLUSION

This article intended to check the machinability performances of AISI D2 steel using coated cermet tool under MQL assisted coconut oil-based trihexyltetradecylphosphonium chloride [$[CH_3(CH_2)_5]P(Cl)(CH_2)_{13}CH_3$] ionic fluid condition. Further, TOPSIS is utilised to find the optimum set of parameters to get the optimum machinability responses. Linear models are also included to correlate the individual response with multi-input parameters. Based on the above, the following concluding remarks are summarised as follows:

i. Coconut oil-based trihexyltetradecylphosphonuium chloride (1% weight) ionic fluid attributes the better quality of finish as Ra varies in between 0.2- 1.82 μm, therefore the implementation of coconut oil-based trihexyltetradecylphosphonium chloride ionic fluid through MQL in machining hardened steel is imperative. Feed rate and depth of cut have equally influenced the Ra with each of them contributed 48.98%.
ii. 1% weight of trihexyltetradecylphosphonium chloride doesn't attribute any significant benefit for flank wear concern, therefore higher % weight concentration of ionic fluid is recommended for further study. Cutting speed attributed the strong influence on flank wear with 90.1 % contribution. Abrasion, chipping, groove wear, and catastrophic tool tip breakage are identified as major tool failure mechanisms.

iii. The MRR is strongly influenced by cutting speed (69.39 %) followed by feed rate (28.94%) due to this highest MRR (1.817g/s) is achieved at the highest cutting speed (180 m/min) and feed (0.18 mm/rev) cutting condition.

iv. Chip shape is strongly affected by feed rate while colour of the chip is highly affected by cutting speed. Helical, ribbon and broken c-type chips shape are noticed while colours are either metallic or blue. Chip reduction coefficient is strongly influenced by the depth of cut (63.4%) succeeded by feed (28.8%).

v. TOPSIS estimated the optimum level of parameters: *d*1 (0.2 mm) - *f*2 (0.12 mm/rev) - *v*2 (120 m/min) and at this condition closeness coefficient (CCo) is improved by 67.1% from initial setting.

vi. Linear regression model effectively co-relate the output and input terms with higher % of R-Square, R-Square(adj) and R-Square(Pred).

Further, the research requires to consider different ionic liquids concentrations. Also, optimisation is required to get the suitable combinations of ionic fluid concentration. Study the effects of other ionic liquids with varying combinations of cation-anion are required for various tool-metal workpiece pairs. The different base oil can also be chosen to study the lubricating and cooling ability of ionic fluid in machining.

ACKNOWLEDGEMENT

The authors express their gratitude to KIIT Deemed to be University, Bhubaneswar, India for carrying out the current research work.

REFERENCE

[1] Agarwal A, Singh, Kumar P, Singh M. Optimization of multiple quality characteristics for CNC turning under cryogenic cutting environment using desirability function. Journal of Materials Processing Technology 2008; 205(1-3): 42-50.

[2] Agrawal SM, Patil NG. Experimental study of non edible vegetable oil as a cutting fluid in machining of M2 steel using MQL. Procedia Manufacturing 2018; 20:207-212.

[3] Balioti V, Tzimopoulos C, Evangelides, C. Multi-criteria decision making using TOPSIS method under fuzzy environment. application in spillway selection. In Multidisciplinary Digital Publishing Institute Proceedings 2018; 2: 637.

[4] Belluco W, De Chiffre L Performance evaluation of vegetable-based oils in drilling austenitic stainless steel. Journals of Material Processing and Technology 2004; 148:171-176.

[5] Bennett EO. Water based cutting fluids and human health. Tribology International 1983; 16(3):133-136.

[6] Bhuyan RK, Routara BC, Parida AK. An approach for optimization the process parameter by using TOPSIS Method of Al–24% SiC metal matrix composite during EDM. Materials Today: Proceedings 2015; 2(4-5):3116-3124.

[7] Byrne G, Dornfeld D, Denkena B. Advancing cutting technology. CIRP Annals 2003; 52(2):483-507.

[8] Cetin MH, Ozcelik B, Kuram E, Demirbas, E. Evaluation of vegetable based cutting fluids with extreme pressure and cutting parameters in turning of AISI 304L by Taguchi method. Journal of Cleaner Production 2011; 19(17-18): 2049-2056.

[9] Chattopadhyay AB. Machining and Machine Tools, 2nd ed., Willey, 2017.

[10] Das A, Mukhopadhyay A, Patel SK, Biswal BB. Comparative assessment on machinability aspects of AISI 4340 alloy steel using uncoated carbide and coated cermet inserts during hard turning. Arabian Journal for Science and Engineering 2016; 41(11):4531-4552.

[11] Das A, Patel SK, Das SR. Performance comparison of vegetable oil based nanofluids towards machinability improvement in hard turning of HSLA steel using minimum quantity lubrication. Mechanics and Industry 2019; 20:506.

[12] Davis B, Schueller JK, Huang Y. Study of ionic liquid as effective additive for minimum quantity lubrication during titanium machining. Manufacturing Letters 2015; 5:1-6.

[13] De Souza MC, Gonçalves JFdS, Gonçalves PC, Lutifd SYS, Gomese JdO. Use of Jatropha and Moringa oils for lubricants: Metalworking fluids more environmental-friendly. Industrial Crops and Products 2019; 129:594–603.

[14] Del Sol I, Gámez AJ, Rivero A, Iglesias P. Tribological performance of ionic liquids as additives of water-based cutting fluids. Wear 2019; 426:845-852.

[15] Dhar N R, Islam MW, Islam S, Mithu MAH. The influence of minimum quantity of lubrication (MQL) on cutting temperature, chip and dimensional accuracy in turning AISI-1040 steel. Journal of Materials Processing Technology 2006; 171(1):93-99.

[16] Dong PQ, Duc TM, Long TT. Performance evaluation of MQCL hard milling of SKD 11 tool steel using MoS2 Nanofluid. Metals 2019; 9:658.

[17] Duc TM, Long TT, Chien TQ. Performance evaluation of MQL parameters using Al2O3 and MoS2 nanofluids in hard turning 90CrSi Steel. Lubricants 2019; 7:40. Doi:10.3390/lubricants7050040

[18] Fernando WLR, Sarmilan N, Wickramasinghe KC, Herath HMCM, Perera GIP. Experimental investigation of minimum quantity lubrication (MQL) of coconut oil based Metal Working Fluid. Materials Today: Proceedings (2019) doi.org/10.1016/j.matpr.2019.06.079

[19] Fox, MF, Priest M. Tribological properties of ionic liquids as lubricants and additives. Part 1: synergistic tribofilm formation between ionic liquids and tricresyl phosphate. Proceedings of the Institution of Mechanical Engineers, Part J: Journal of Engineering Tribology 2008; 222(3):291-303.

[20] Goindi GS, Chavan SN, Mandal D, Sarkar P, Jayal AD. Investigation of ionic liquids as novel metalworking fluids during minimum quantity lubrication machining of a plain carbon steel. Procedia CIRP 2015; 26:341-345.

[21] Goindi GS, Jayal AD, Sarkar P. Application of ionic liquids in interrupted minimum quantity lubrication machining of plain medium carbon steel: Effects of ionic liquid properties and cutting conditions. Journal of Manufacturing Processes 2018; 32:357-371.

[22] Gutnichenko O, Bushlya V, Bihagen S, Stahl J-E. Influence of graphite nanoadditives to vegetable-based oil on machining performance when MQCL assisted hard turning. Procedia CIRP 2018; 77:437-440.

[23] KC Anil, Vikas MG, BT Shanmukha, Rao KVS. Effect of cutting parameters on surface finish and machinability of graphite reinforced Al-8011 matrix composite. IOP Conf. Series: Materials Science and Engineering 2017; 191:012025.

[24] Kumar R, Sahoo AK, Mishra PC, Das RK. Investigation on Tool Wear and Surface Characteristics in Hard Turning Under Air-Water Jet Spray Impingement Cooling Environment. Tribology In Industry 2019; 41(2): 172-187.

[25] Kumar R, Sahoo AK, Mishra PC, Das RK, Ukamanal M. Experimental investigation on hard turning using mixed ceramic insert under accelerated cooling environment. International Journal of Industrial Engineering Computations 2018; 9(4):509-522.

[26] Kumar R, Sahoo AK, Mishra PC, Das RK. Measurement and machinability study under environmentally conscious spray impingement cooling assisted machining. Measurement 2019; 135:913-927.

[27] Kumar R, Sahoo AK, Mishra PC, Das RK. Performance of Near Dry Hard Machining Through Pressurised Air Water Mixture Spray Impingement Cooling Environment. International Journal of Automotive and Mechanical Engineering 2019; 16(1):6108-6133.

[28] Kumar R, Sahoo AK, Mishra PC, Das RK. Comparative investigation towards machinability improvement in hard turning using coated and uncoated carbide inserts: part I experimental investigation. Advances in Manufacturing 2018; 6(1):52-70.

[29] Kumar R, Sahoo AK, Mishra PC, Das RK. Comparative study on machinability improvement in hard turning using coated and uncoated carbide inserts: part II modeling, multi-response optimization, tool life, and economic aspects. Advances in Manufacturing 2018; 6(2):155-170.

[30] Liu XQ, Zhou F, Liang, YM, Liu, W. Benzotriazole as the additive for ionic liquid lubricant: one pathway towards actual application of ionic liquids. Tribology Letters 2006; 23(3):191-196.

[31] Merugu Rakesh, Saurav Datta, Effects of Cutting Speed on Chip Characteristics and Tool Wear Mechanisms During Dry Machining of Inconel 718 Using Uncoated WC Tool, Arabian Journal for Science and Engineering, https://doi.org/10.1007/s13369-019-03785-y

[32] Minami I, Kamimura H, Mori S. Thermo-oxidative stability of ionic liquids as lubricating fluids. Journal of Synthetic Lubrication 2007; 24(3):135-147.

[33] Mukherjee S, Kamal A, Kumar K. Optimization of material removal rate during turning of SAE 1020 material in CNC lathe using Taguchi technique. Procedia Engineering 2014; 97:29–35.

[34] Nune MMR, Chaganti PK (2019) Development, characterization, and evaluation of novel eco-friendly metal working fluid. Measurement 2019; 137:401–416.

[35] Panda A, Sahoo AK, Panigrahi I, Rout AK. Investigating machinability in hard turning of AISI 52100 bearing steel through performance measurement: QR, ANN and GRA Study. International Journal of Automotive and Mechanical Engineering 2018; 15:4935-4961.

[36] Park KH, Olortegui-Yume J, Yoon MC, Kwon P. A study on droplets and their distribution for minimum quantity lubrication (MQL). International Journal of Machine Tools and Manufacture 2010; 50(9):824-833.

[37] Pereira O, Català P, Rodríguez A, Ostra T, Vivancos J, River, A, López-de-Lacalle LN. The use of hybrid CO2+MQL in machining operations. Procedia Engineering 2015; 132:492-499.

[38] Phillips BS, John G, Zabinski JS. Surface chemistry of fluorine containing ionic liquids on steel substrates at elevated temperature using Mössbauer spectroscopy. Tribology Letters 2007; 26(2):85-91.

[39] Qu J, Bansal DG, Yu B, Howe JY, Luo H, Dai S. Smolenski DJ. Antiwear performance and mechanism of an oil-miscible ionic liquid as a lubricant additive. ACS Applied Materials & Interfaces 2012; 4(2):997-1002.

[40] Qu J, Luo H, Chi M, Ma C, Blau PJ, Dai S, Viola MB. Comparison of an oil-miscible ionic liquid and ZDDP as a lubricant anti-wear additive. Tribology International 2014; 71:88-97.

[41] Qu J, Truhan JJ, Dai S, Luo H, Blau PJ. Ionic liquids with ammonium cations as lubricants or additives. Tribology Letters 2006; 22(3):207-214.

[42] Ramesh S, Viswanathan R, Ambika S. Measurement and optimization of surface roughness and tool wear via grey relational analysis, TOPSIS and RSA techniques. Measurement 2016; 78:63-72.

[43] Sahoo AK, Sahoo B. Performance studies of multilayer hard surface coatings (TiN/TiCN/Al2O3/TiN) of indexable carbide inserts in hard machining: Part-I (An experimental approach). Measurement 2013; 46:2854-2867.

[44] Sani ASA, Rahim EA, Sharif S, Sasahara H. The influence of modified vegetable oils on tool failure mode and wear mechanisms when turning AISI 1045. Tribology International 2019; 129:347–362.

[45] Sani ASA, Rahim EA, Talib N, Kamdani K, Rahim MZ, Samion S. Performance evaluation of palm-olein TMP ester containing hexagonal boron nitride and an oil miscible ionic liquid as bio-based metalworking fluids. Journal of Mechanical Engineering 2017; 4(1):223-234.

[46] Sani, ASA, Rahim EA, Sharif S, Sasahara H. Machining performance of vegetable oil with phosphonium-and ammonium-based ionic liquids via MQL technique. Journal of Cleaner Production 2019; 209:947-964.

[47] Spikes H. Friction modifier additives. Tribology Letters (2015) 60(1):5.

[48] Upadhyay V, Jain PK, Mehta NK, Branko K. Minimum quantity lubrication assisted turning—an overview: Daaam International Scientific Book 2012; 463-478.

[49] Weinert, K, Inasaki, I, Sutherland, JW, Wakabayashi, T. Dry machining and minimum quantity lubrication. CIRP annals 2004; 53(2): 511-537.

[50] Weng L, Liu X, Liang Y, Xue Q. Effect of tetraalkylphosphonium based ionic liquids as lubricants on the tribological performance of a steel-on-steel system. Tribology Letters 2017; 26(1):11-17.

[51] Ye C, Liu W, Chen Y, Yu L. Room-temperature ionic liquids: a novel versatile lubricant. Chemical Communications 2001; 21:2244-2245.

[52] Yousefi S, Zohoor M. Effect of cutting parameters on the dimensional accuracy and surface finish in the hard turning of MDN250 steel with cubic boron nitride tool, for developing a knowledged base expert system. International Journal of Mechanical and Materials Engineering 2019;14-1.

[53] Zhou Y, Qu J. Ionic liquids as lubricant additives: a review. ACS Applied Materials & Interfaces 2017; 9(4):3209-3222.